4. Daling JR, Madeleine MM, Schwartz SM *et al.* A population-based study of squamous cell vaginal cancer: HPV and cofactors. *Gynecol Oncol* 2002;**84**:263–70.

5. Greene FL, Page DL, ID F. *Gynecologic Sites: Vagina AJCC Cancer Staging Manual,* 6th edn. New York: Springer, 2002, 255–8.

6. Nakano T, Kato S, Ohno T *et al.* Long-term results of high-dose rate intracavitary brachytherapy for squamous cell carcinoma of the uterine cervix. *Cancer* 2005;**103**:92–101.

7. Toita T, Kato S, Niibe Y *et al.* Prospective multi-institutional study of definitive radiotherapy with high-dose-rate intracavitary brachytherapy in patients with nonbulky (<4-cm) stage I and II uterine cervical cancer (JAROG0401/JROSG04-2). *Int J Radiat Oncol Biol Phys* 2012;**82**:e49–56.

8. Itami J, Hara R, Kozuka T *et al.* Transperineal high-dose-rate interstitial radiation therapy in the management of gynecologic malignancies. *Strahlenther Onkol* 2003;**179**:737–41.

9. Kaplan EL, Meier P. Nonparametric estimation from incomplete observations. *J Amer Statist Assoc* 1958;**53**:457–81.

10. Bland JM, Altman DG. The logrank test. *BMJ* 2004;**328**:1073.

11. Frank SJ, Jhingran A, Levenback C *et al.* Definitive radiation therapy for squamous cell carcinoma of the vagina. *Int J Radiat Oncol Biol Phys* 2005;**62**:138–47.

12. Leung S, Sexton M. Radical radiation therapy for carcinoma of the vagina—impact of treatment modalities on outcome: Peter MacCallum Cancer Institute experience 1970-1990. *Int J Radiat Oncol Biol Phys* 1993;**25**:413–8.

13. Nonaka T, Nakayama Y, Mizoguchi N *et al.* (7 February 2012) Definitive radiation therapy for invasive carcinoma of the vagina: impact of high-dose rate intracavitary brachytherapy. *Int J Clin Oncol,* 10.1007/s10147-012-0379-7.

14. Seeger AR, Windschall A, Lotter M *et al.* The role of interstitial brachytherapy in the treatment of vaginal and vulvar malignancies. *Strahlenther Onkol* 2006;**182**:142–8.

15. Hegemann S, Schafer U, Lelle R *et al.* Long-term results of radiotherapy in primary carcinoma of the vagina. *Strahlenther Onkol* 2009;**185**:184–9.

16. Beriwal S, Demanes DJ, Erickson B *et al.* American Brachytherapy Society consensus guidelines for interstitial brachytherapy for vaginal cancer. *Brachytherapy* 2012; **11**:68–75.

17. Chyle V, Zagars GK, Wheeler JA *et al.* Definitive radiotherapy for carcinoma of the vagina: outcome and prognostic factors. *Int J Radiat Oncol Biol Phys* 1996; **35**:891–905.

❖ Scientific
❖ Research

Usefulness of Immuno-Magnetic Beads Conjugated with Anti-EpCAM Antibody for Detecting Endometrial Cancer Cells[*]

Yoshikatsu Koga[1], Satoshi Katayose[2], Nobuko Onoda[2], Takahiro Kasamatsu[3], Tomoyasu Kato[3], Shunichi Ikeda[3], Mitsuya Ishikawa[3], Ken Ishitani[4], Yasuo Hirai[4], Hideo Matsui[4], Yasuhiro Matsumura[1]

[1]Division of Developmental Therapeutics, Research Center for Innovative Oncology, National Cancer Center Hospital East, Kashiwa, Japan; [2]R & D Department Unit 1, JSR Life Sciences Corporation, Tsukuba, Japan; [3]Department of Gynecology, National Cancer Center Hospital, Tokyo, Japan; [4]Department of Obstetrics and Gynecology, Tokyo Women's Medical University, Tokyo, Japan.
Email: yhmatsum@east.ncc.go.jp

ABSTRACT

A simple and non-invasive method for detecting endometrial cancer in women with abnormal uterine bleeding is required. For this purpose, we prepared immuno-magnetic beads conjugated with anti-human EpCAM rat monoclonal antibody (mAb) for isolating exfoliated endometrial cells including endometrial cancer cells in vaginal discharge. The affinities of the anti-human EpCAM rat mAbs were analyzed by flow cytometry and immunocytochemistry and then magnetic beads were conjugated with the mAbs. The rate of retrieval of endometrial cells using the immuno-magnetic beads was calculated. Endometrial cells were isolated using the immuno-magnetic beads from the vaginal discharges of 22 patients with endometrial cancer and 16 non-malignant controls. The isolated cells were stained using endometrial cancer specific-mAbs and analyzed by flow cytometry and imaging cytometry. The immuno-magnetic beads conjugated with high-affinity mAb (clone 1456) appeared to have very low auto-fluorescence. Sufficient enrichment of Ep-CAM-positive cells using immuno-magnetic beads was observed in both simulation and clinical samples. The overall sensitivities of flow cytometry and imaging cytometry to detect endometrial cancer cells were 72.7% and 45.5%, respectively. Meanwhile, the overall specificities of flow cytometry and imaging cytometry for healthy controls were 75.0% and 81.3%, respectively. Our immuno-magnetic beads have very low auto-fluorescence, so they could be useful for fluorescent analysis, such as fluorescent immunochemical staining. In the future, these novel immuno-magnetic beads could be used for cytological study.

Keywords: Immuno-Magnetic Beads; Auto-Fluorescence; Endometrial Cancer; Cancer Screening

1. Introduction

Endometrial cancer is one of the most common malignancies of the female genital tract globally [1]. In the USA, approximately 80% of patients with cancer of the uterus were diagnosed as having endometrial cancer [2] and the number of patients with endometrial cancer has been increasing in Japan [3]. Regarding cancer screening of female genital cancers, cervical cancer of the uterus can be diagnosed more simply than endometrial cancer [4]. However, there is no screening method for endometrial cancer at present [5]. Abnormal uterine bleeding is a common symptom of endometrial cancer; however, endometrial cancer is diagnosed in only 10% of women with abnormal uterine bleeding [6,7] and no organic cause is found in 60% to 70% of these women [8]. For many years, dilatation followed by curettage has been the standard method for detecting endometrial cancer in women with abnormal uterine bleeding. In the last decade, several screening methods for women with abnormal uterine bleeding, such as transvaginal sonography [9,10], endometrial cytology [10], suction endometrial curettage [10], and endometrial sampling [10,11], were reported to reduce the cost and invasiveness. However, these screening methods are still invasive, time-con-

suming, and expensive, and above all, inconvenient for women. Therefore, a simple, economic, and non-invasive method of detecting cancer through cancer screening for patients with abnormal uterine bleeding is required.

Recently, we reported a cytological analysis for the detection of endometrial cancer cells combined with endometrial cancer-specific monoclonal antibodies (mAbs) and imaging cytometry using exfoliated endometrial cells [12]. Exfoliated endometrial cancer cells and normal endometrial cells were observed in the vaginal discharge of patients with endometrial cancer. In addition, to detect endometrial cancer cells, mAbs against cysteine-rich with EGF-like domain 1 (CRELD1), G-protein-coupled receptor kinase 5 (GRK5), solute carrier family 25 member 27 (SLC25A27), and stanniocalcin 2 (STC2) were used. However, almost all tampon-retrieved cells were granulocytes and normal squamous cells from the vagina, and the rate of endometrial cells in all tampon-retrieved cells was less than 1% [12].

Meanwhile, to isolate exfoliated colonocytes from feces, we previously reported immuno-magnetic beads conjugated with anti-human epithelial cell adhesion molecule (EpCAM) mouse mAb (Magnosphere MC290/anti-EpCAM mouse IgG, JSR Life Sciences, Tsukuba, Japan) [13]. The same as for fecal samples, exfoliated endometrial cells could be isolated using immuno-magnetic beads. The capturing mAbs (anti-human EpCAM mAbs conjugated to Magnosphere) and the detecting mAbs (endometrial cancer-specific mAbs) are both mouse monoclonal antibodies; thus, the secondary antibody for immunochemical staining cross-reacted with the mAbs for capture and those for detection. To resolve this issue, we have established anti-human EpCAM rat mAb and immuno-magnetic beads with very low auto-fluorescence for the isolation of exfoliated endometrial cells in the present study. Then, the exfoliated endometrial cells collected using immuno-magnetic beads were subjected to cellular analysis.

2. Materials and Methods

2.1. Establishment of Anti-Human EpCAM Rat Monoclonal Antibodies

A recombinant human EpCAM/Fc chimera (R & D Systems, Minneapolis, MN) was used as an immunogen. 0.1 mg of the antigen was mixed with complete Freund's adjuvant (Difco, Detroit, MI) and injected intraperitoneally into Wistar rat (Japan SLC, Shizuoka, Japan). The ELISA-positive hybridoma cells were cloned by limiting dilution in 96-well culture plates and established as stable hybridoma cells.

Immunoglobulin G was separately purified from each ascites fluid sample using protein G affinity chromatog-

raphy (GE Healthcare Life Science, Piscataway, NJ). The purified IgG fractions were used for further characterization and were evaluated for their reactivity.

2.2. Flow Cytometry of Anti-Human EpCAM mAb

HT-29 cells and UMUC-3 cells were used as EpCAM-positive and -negative cells, respectively. 2×10^5 trypsinized cells were put into a 2-mL tube and incubated with 0.2 µg of each mAb for 30 min at 4°C. After rinsing with PBS containing 0.5% bovine serum albumin (BSA) and 2 mM ethylenediaminetetraacetic acid (EDTA) (B. E. PBS), the cells were incubated with 0.1 µg of DyLight 649-conjugated donkey anti-rat IgG secondary antibody (Jackson ImmunoResearch, West Grove, PA) for 30 min at 4°C. Finally, the cells were rinsed with B. E. PBS and nuclear-stained with propidium iodide (PI) solution (Invitrogen, Eugene, OR). The stained cells were analyzed by flow cytometry using a Guava easyCyte.

2.3. Immunocytochemistry of Anti-Human EpCAM mAb

EpCAM-positive and -negative cells were pre-cultured on BD Falcon culture slides (BD Biosciences, Bedford, MA). The cells were fixed in 4% paraformaldehyde (Wako, Osaka, Japan) for 30 min at 4°C and rinsed with ultrapure water. Endogenous peroxidase was blocked with a 3% hydrogen peroxide solution in 100% methanol for 30 min at room temperature, followed by rinsing with PBS. Nonspecific protein binding was blocked with 5% skim milk in PBS for 30 min at room temperature. After draining off the skim milk solution, the cells were incubated with 4 µg of each anti-human EpCAM rat mAb for 1 hr at room temperature. After rinsing with PBS, the cells were incubated with 0.1 µg of HRP-conjugated donkey anti-rat IgG secondary antibody (Jackson ImmunoResearch) for 30 min at room temperature. After rinsing with PBS, the cells were incubated with the 3,3'-diaminobenzidine tetrahydrochloride (DAB+) liquid system (Dako, Glostrup, Denmark) for 5 min at room temperature. Finally, the cells were rinsed and counter-stained with hematoxylin solution.

2.4. Immuno-Magnetic Beads Conjugated with Anti-Human EpCAM Rat mAb

Magnetic beads of 3.0 µm diameter, Magnosphere MC290/Tosyl (JSL Life Sciences), were prepared in this study. The magnetic beads were directly conjugated with anti-human EpCAM rat mAb. The sizes of the obtained magnetic beads were determined to be 3.0 µm based on electron microscopic observation. Also, commercially available immuno-magnetic beads conjugated with anti-

human EpCAM mouse mAb, Dynabeads Epithelial Enrich (Dynal, Oslo, Norway) and Magnosphere MC290/anti-EpCAM mouse IgG (JSR Life Sciences), were used in the present study.

2.5. Simulation Analysis for Retrieving Cells Using Immuno-Magnetic Beads

In the present study, the immuno-magnetic beads were used for the isolation of endometrial cells from the samples of abnormal uterine bleeding or menstrual bleeding; thus, EpCAM-positive cells added to peripheral blood were used in the simulation study. 1×10^6 HT-29 cells with 3 mL of peripheral blood (approximately 1×10^7 granulocytes) were prepared in the simulation study. 30 mL of a retrieval PBS buffer containing 0.1% BSA and 2 mM EDTA was added to the sample. The EpCAM-positive cells were captured using 40 μL of immuno-magnetic beads, and the mixtures were incubated for 30 min under gentle rolling at room temperature. Then, the mixtures on the magnet were incubated on a shaking platform for 15 min at room temperature. Subsequently, the supernatant was removed and the retrieved cells were fixed in 4% paraformaldehyde for 30 min at 4°C. In the clinical simulation study, menstrual blood from a healthy volunteer was subjected to the same method as described above.

To analyze the efficiency of immuno-magnetic beads, the cells retrieved using the immuno-magnetic beads were stained with the anti-human EpCAM goat polyclonal Ab (R & D Systems) and assessed using an imaging cytometer, CELAVIEW (Olympus, Tokyo, Japan). The retrieved cells were plated into each well of flat-bottomed 96-well tissue culture plates (Corning). The plates were centrifuged at 30 g for 5 min at 4°C and the supernatant was removed, followed by drying over-night at room temperature. The cells were permeabilized by incubation in PBS containing 0.2% Triton X-100 for 20 min at room temperature. Non-specific protein binding was blocked with 5% skim milk in PBS for 30 min at room temperature. After draining off the skim milk solution, the cells were incubated with 1 μg of commercially available anti-human EpCAM goat polyclonal Ab, followed by incubation for 1 hr at room temperature. After rinsing with PBS, the sections were incubated with 0.1 μg of DyLight 488-conjugated bovine anti-goat IgG secondary antibody (Jackson ImmunoResearch) for 30 min at room temperature.

2.6. Patients with Endometrial Cancer or Non-Malignant Controls

From January 2012 to December 2012, 22 patients with histologically confirmed endometrial cancer and 16 non-

malignant controls before menopause were enrolled in this study (**Table 1**). All the patients had undergone surgical resection of their primary cancer at the National Cancer Center Hospital, Tokyo, Japan. The endometrial cancer patients were slightly older than the non-malignant controls. All patients and controls received detailed information about the study and gave written consent to participate in the study, which was approved by the Institutional Review Board of the National Cancer Center, Japan, and Tokyo Women's Medical University.

2.7. Retrieval of Naturally Exfoliated Endometrial Cells Using Immuno-Magnetic Beads

The participants in this study inserted a small tampon (3 × 1 cm, Unicharm, Tokyo, Japan) into their vagina and took the tampon out after about 3 hrs [12]. The tampon was then placed in a centrifuge tube (Corning) containing 30 mL of retrieval buffer and was shipped immediately to our laboratory at 4°C. To retrieve the exfoliated cells from the tampon, it was pressed thoroughly and all

Table 1. Characteristics of endometrial cancer patients and non-malignant controls.

	Patients (N = 22)	Controls (N = 16)
Age [median (range)]	60 (47 - 75)	41 (29 - 52)
EpCAM + cells FCM [median (range)]	17 (1 - 2322)	113 (2 - 1964)
EpCAM + cells ICM [median (range)]	17 (0 - 1893)	82 (0 - 2014)
Histology [Number (%)]		
Endometrioid adenocarcinoma	18 (81.8%)	
Mixed adenocarcinoma	2 (9.1%)	
Serous adenocarcinoma	1 (4.5%)	
Carcinosarcoma	1 (4.5%)	
FIGO classification [Number (%)]		
stage I	14 (63.6%)	
stage II	4 (18.2%)	
stage III	3 (13.6%)	
stage IV	1 (4.5%)	
Tumor size [mm, median (range)]	37 (9 - 82)	

Patients: patients with endometrial cancer, Controls: non-malignant patients without malignancy in the uterus, EpCAM + cells FCM: positively stained cells using EpCAM Ab counted by flow cytometry, EpCAM + cells ICM: positively stained cells using EpCAM Ab counted by imaging cytometry, FIGO: International Federation of Gynecology and Obstetrics.

obtained fluid was collected in another new centrifuge tube. The exfoliated endometrial cells were captured by adding 40 μL of immuno-magnetic beads into the sample solution, and the mixtures were incubated for 30 min under gentle rolling conditions at room temperature. The mixtures on the magnet were incubated on a shaking platform for 15 min at room temperature. Then, the supernatant was removed and the retrieved cells were fixed in 4% paraformaldehyde for 30 min at 4°C. The cells were rinsed with PBS and stored in 1 mL of PBS-based storage buffer containing 0.1% BSA, 2 mM EDTA, and 0.1% NaN3 at 4°C until analysis.

2.8. Cellular Analysis Using Flow Cytometry and Imaging Cytometry

For cellular analysis using flow cytometry, the exfoliated endometrial cells retrieved using the immuno-magnetic beads were put into a 2-mL tube and incubated with 4 μg of anti-CRELD1 (clone 2D1E12I), GRK5 (clone 2F11C3), SLC25A27 (clone 3A8B14), and STC2 (clone 2D4C4) mouse mAbs (ACTGen, Nagano, Japan) as well as 1 μg of anti-human EpCAM goat polyclonal antibody for 1 hr at room temperature. After rinsing with retrieval buffer, the cells were incubated with 0.1 μg of DyLight 488-conjugated bovine anti-goat IgG secondary antibody and 0.1 μg of DyLight 649-conjugated donkey anti-mouse IgG secondary antibody for 30 min at room temperature. Finally, the cells were rinsed with retrieval buffer and nuclear-stained with PI solution. The stained cells were analyzed using flow cytometry with a Guava easyCyte (Millipore, Billerica, MA).

For cellular analysis using imaging cytometry, the exfoliated endometrial cells retrieved using immuno-magnetic beads were prepared as described in the simulation experiment.

3. Results

3.1. Evaluation of Anti-Human EpCAM Rat Monoclonal Antibodies

Mean intensities of EpCAM positive cells with isotype control (negative control), clone B8-4 (positive control), clone 118, clone 533, clone 572, clone 787, clone 1097, clone 1286, clone 1456, and clone 1468 were 3.33, 1683, 1823, 810, 1865, 1693, 1571, 1531, 1670, and 861, respectively (Figure 1(a)). Mean intensities of EpCAM-negative cells with the same mAbs were 3.54, 3.75, 5.00, 3.52, 3.92, 12.9, 5.41, 6.33, 3.58, and 3.24, respectively (Figure 1(b)). The affinities to EpCAM-positive cells using two mAbs (clones 533 and 1468) were lower than that to clone B8-4. Meanwhile, non-specific reactions to EpCAM-negative cells were observed for four mAbs (clones 118, 787, 1097, and 1286). From the results of

flow cytometry, two mAbs (clones 572 and 1456) were selected as candidates for the conjugation. In the immunocytochemical staining, EpCAM-positive cells were stained positively by clone B8-4 and clone 1456 mAbs (Figure 1(c)). However, these cells could not be stained by clone 572 mAb. Thus, clone 1456 was used as anti-human EpCAM rat mAb in the following experiments.

3.2. Low Auto-Fluorescence of Immuno-Magnetic Beads Conjugated with Anti-Human EpCAM Rat mAb

The levels of auto-fluorescence of commercially available immuno-magnetic beads (Dynabeads Epithelial Enrich and MC290/EpCAM mouse IgG) and our new immuno-magnetic beads (MC290/EpCAM rat IgG) were compared (Figure 2(a)). Fluorescent intensities were assessed at wavelengths of excitation (Ex) 488 nm/emission (Em) 525 nm (green fluorescence), Ex 488 nm/Em 583 nm (yellow fluorescence), Ex 488 nm/Em 680 nm (red fluorescence), and Ex 640 nm/Em 661 nm (red2 fluorescence). Mean intensities of Dynabeads Epithelial Enrich in terms of green, yellow, red, and red2 fluorescence were 13.7, 41.5, 44.3, and 10.8, respectively. Corresponding mean intensities of MC290/EpCAM mouse IgG were 3.01, 4.61, 4.05, and 6.03, respectively. In addition, mean intensities of MC290/EpCAM rat IgG were 2.82, 4.20, 3.29, and 6.35, respectively. Consequently, MC290 beads showed low auto-fluorescence and Dynabeads showed high auto-fluorescence. The binding of Dynabeads and MC290 beads to EpCAM-positive cells
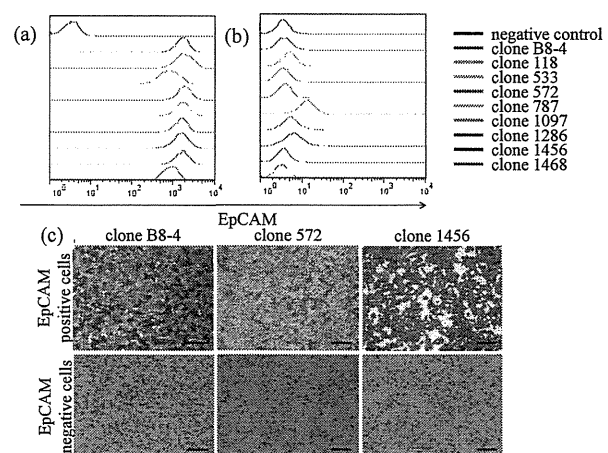
Figure 1. Evaluation of anti-human EpCAM rat monoclonal antibodies. (a) Flow cytometry using EpCAM-positive cells. Seven clones of anti-human EpCAM rat mAbs were compared to a positive control (anti-human EpCAM mouse mAb; clone B8-4). (b) Flow cytometry using EpCAM-negative cells. (c) Immunocytochemistry of EpCAM-positive and -negative cells using clone B8-4, clone 1456, and clone 572. Scale bar represents 100 μm.

is shown in **Figure 2(b)**. EpCAM-positive cells were retrieved by using both Dynabeads Epithelial Enrich and MC290 beads; however, Dynabeads showed auto-fluorescence. Meanwhile, MC290 had the lowest level of auto-fluorescence. Thus, our MC290/EpCAM rat IgG appeared to be useful for fluorescent immunochemistry.

3.3. Cell Isolation Using Immuno-Magnetic Beads Conjugated with Anti-Human EpCAM Rat mAb

In the simulation experiment, EpCAM-positive cells were added to granulocytes at a ratio of approximately 1:10. The actual proportion of EpCAM-positive cells was 8.8% (EpCAM-positive cells/all cells: 659/7508) (**Figures 3(a) and (e)**). After the isolation using the beads, the rate of EpCAM-positive cells was 48.5% (306/634) (**Figures 3(b) and (f)**). In the clinical sample, menstrual blood of a healthy volunteer was used. The rate of EpCAM-positive cells in the clinical subject was 3.0% (361/12,112) (**Figures 3(c) and (g)**). After the isolation using the beads, the rate of EpCAM-positive cells in the clinical subject was 61.9% (224/394) (**Figures 3(d) and (h)**). Recovery rate of EpCAM-positive cells using immuno-magnetic beads was 50% to 67%. Thus, EpCAM-positive cells before cell isolation were more than that after cell isolation. All cells were stained by DAPI (blue) and EpCAM-positive

cells were stained by anti-EpCAM mAb (green) and DAPI (blue). After cell isolation, many particles without staining as shown in the **Figures 3(f) and (h)** were immuno-magnetic beads. Sufficient enrichment of EpCAM-positive cells using MC290/EpCAM rat IgG was thus observed in both the simulation experiment and the clinical samples.

3.4. Clinical Evaluation of Cellular Analysis

The median numbers of EpCAM-positive cells observed in endometrial cancer patients using flow cytometry and imaging cytometry were 17 (range 1 - 2322) and 17 (0 - 1893), respectively. Meanwhile, the median numbers of EpCAM-positive cells observed in healthy controls using flow cytometry and imaging cytometry were 113 (range 2 - 1964) and 82 (0 - 2014), respectively. The samples with less than 10 EpCAM-positive cells were not applicable in this study. Samples with over 10 EpCAM-positive cells were examined and for practical purpose, more than 20% positive by the cancer detecting mAbs were designated "positive". The sensitivities and specificities of cellular analyses using flow cytometry and imaging cytometry are shown in **Table 2**. In the flow cytometry, immuno-staining-positive cells using CRELD1, GRK5, SLC25A27, and STC2 mAbs were observed in 40.9%, 18.2%, 18.2%, and 27.3% of endometrial cancer patients,
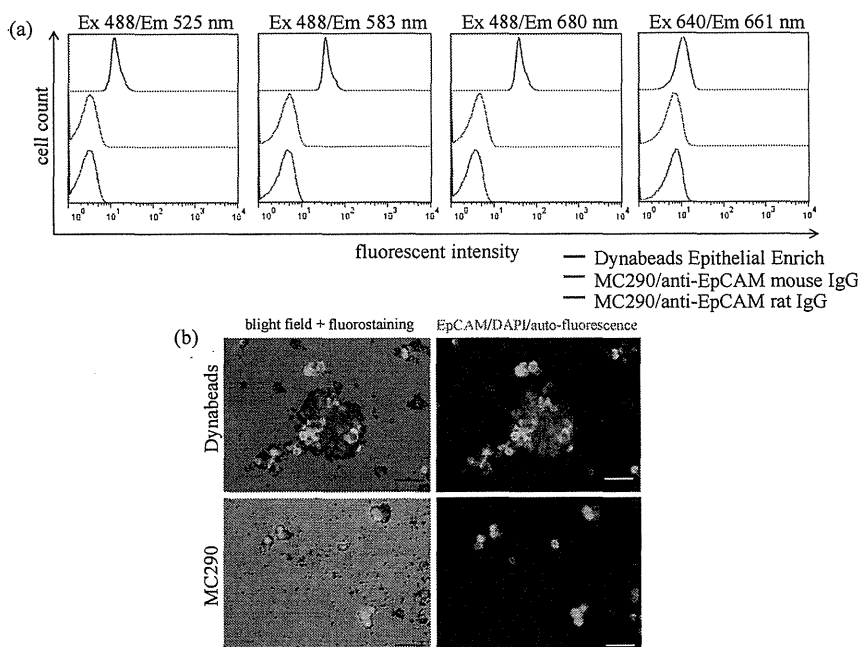

Figure 2. Auto-fluorescence of each bead. (a) Auto-fluorescence of Dynabeads Epithelial Enrich, MC290/EpCAM mouse IgG and MC290/EpCAM rat IgG. Fluorescent intensities were assessed at wavelengths of excitation (Ex) 488 nm/emission (Em) 525 nm, Ex 488 nm/Em 583 nm, Ex 488 nm/Em 680 nm, and Ex 640 nm/Em 661 nm. (b) Binding abilities of Dynabeads and MC290 beads to EpCAM-positive cells. EpCAM-positive cells were retrieved by using both Dynabeads Epithelial Enrich and MC290 beads. Dynabeads exhibited some auto-fluorescence, while MC290 exhibited less. Scale bar represents 100 µm.
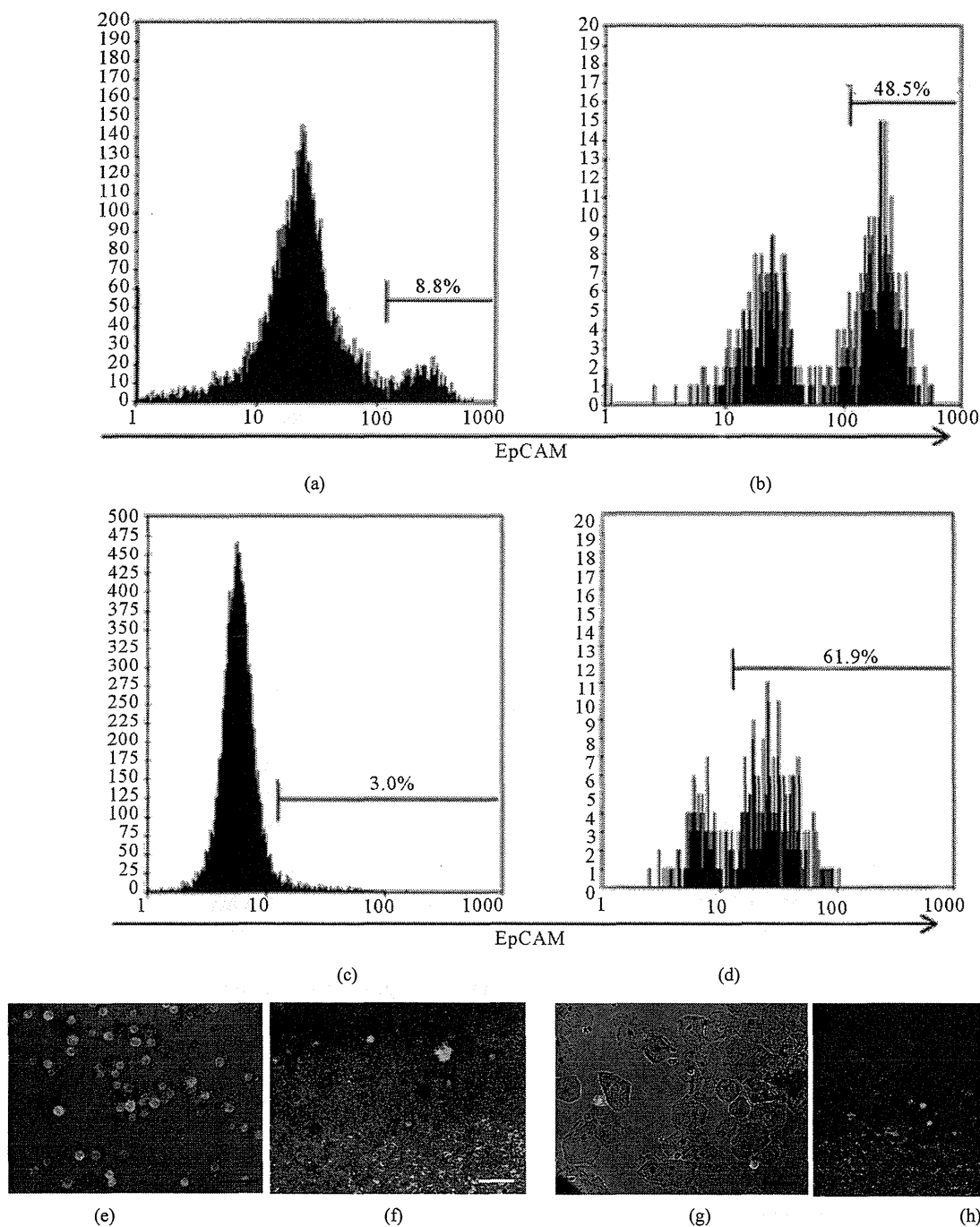
Figure 3. Cell isolation using immuno-magnetic beads tagged with anti-human EpCAM rat mAb. (a) Imaging cytometry of simulation study before cell isolation. The rate of EpCAM-positive cells in the simulation subject before bead isolation was 8.8% (EpCAM-positive cells/all cells: 659/7508). (b) Imaging cytometry of simulation study after cell isolation. The rate of EpCAM-positive cells in the simulation subject after bead isolation was 48.5% (306/634). (c) Imaging cytometry of clinical simulation study before cell isolation. The rate of EpCAM-positive cells in the clinical subject before bead isolation was 3.0% (361/12,112). (d) Imaging cytometry of clinical simulation study after cell isolation. The rate of EpCAM-positive cells in the clinical subject after bead isolation was 61.9% (224/394). (e) Immunocytochemistry of simulation study before cell isolation. (f) Immunocytochemistry of simulation study after cell isolation. (g) Immunocytochemistry of clinical simulation study before cell isolation. (h) Immunocytochemistry of clinical simulation study after cell isolation. EpCAM protein was stained with Dy-Light 488 (green) and the nucleus was stained with DAPI (blue). Scale bar represents 100 μm.

Table 2. Sensitivities and specificities of cellular analyses using flow cytometry and imaging cytometry.

	Endometrial cancer patients (N = 22)			
	Flow cytometry		Imaging cytometry	
	No.	Sensitivity (%, 95% CI)	No.	Sensitivity (%, 95% CI)
Combined marker	16	72.7% (49.8 - 89.3)	10	45.5% (24.4 - 67.8)
CRELD1	9	40.9% (20.7 - 63.7)	4	18.2% (5.2 - 40.3)
GRK5	4	18.2% (5.2 - 40.3)	4	18.2% (5.2 - 40.3)
SLC25A27	4	18.2% (5.2 - 40.3)	2	9.1% (1.1 - 29.2)
STC2	6	27.3% (10.7 - 50.3)	2	9.1% (1.1 - 29.2)
	Non-malignant controls (N = 16)			
	Flow cytometry		Imaging cytometry	
	No.	Specificity (%, 95% CI)	No.	Specificity (%, 95% CI)
Combined marker	12	75.0% (47.7 - 92.7)	13	81.3% (54.3 - 96.0)
CRELD1	14	87.5% (61.7 - 98.5)	15	93.8% (69.8 - 99.8)
GRK5	15	93.8% (69.8 - 99.8)	16	100% (79.4 - 100)
SLC25A27	14	87.5% (61.7 - 98.5)	15	93.8% (69.8 - 99.8)
STC2	15	93.8% (69.8 - 99.8)	14	87.5% (61.7 - 98.5)

CRELD1: cysteine-rich with EGF-like domain 1 (clone 2D1E12I), GRK5: G-protein-coupled receptor kinase 5 (clone 2F11C3), SLC25A27: solute carrier family 25 member 27 (clone 3A8B14), STC2: stanniocalcin 2 (clone 2D4C4), 95% CI: 95% confidence interval.

respectively. In the imaging cytometry, immuno-staining-positive cells using CRELD1, GRK5, SLC25A27, and STC2 mAbs were observed in 18.2%, 18.2%, 9.1%, and 9.1% of endometrial cancer patients, respectively. Approximately 90% of non-malignant controls were negative in both flow cytometry and imaging cytometry using these cancer-specific mAbs. The overall sensitivities of flow cytometry and imaging cytometry to detect endometrial cancer cells were 72.7% [95% confidence interval (CI), 49.8 - 89.3] and 45.5% (95% CI, 24.4 - 67.8), respectively. On the other hand, the overall specificities of flow cytometry and imaging cytometry for non-malignant controls were 75.0% (95% CI, 47.7 - 92.7) and 81.3% (95% CI, 54.3 - 96.0), respectively.

4. Discussion

The tampon retrieval sample contained several kinds of exfoliated cell, such as granulocytes, normal squamous cells, and endometrial cells [12]. Thus, a cell isolation method using immuno-magnetic beads was important for the isolation of exfoliated endometrial cells from tampon. There were two problems regarding the fluorescent immunochemical staining of exfoliated endometrial cells retrieved using immuno-magnetic beads. One was that the fluorescent secondary antibody cross-reacted to both the capturing mAb and the detecting mAb because both

were mouse mAbs. To resolve this issue, we succeeded in developing anti-human EpCAM rat IgG (clone 1456), the affinity of which was as high as that of anti-human EpCAM mouse IgG (clone B8-4). We established clone B8-4 as high affinity mAb in the previous study [13]. Clone B8-4 was useful for immunohistochemistry, flow cytometry, and cell isolation. Thus, we used clone B8-4 as a positive control in this study. We think that clone 572 may recognize protein structure of EpCAM antigen on living cells, thus, this mAb was positive for flow cytometry but negative for immunochemical staining. The other problem to be resolved was the auto-fluorescence of immuno-magnetic beads. The fluorescent intensity cannot be calculated correctly if the immuno-magnetic beads exhibit auto-fluorescence. Polyurethanes are frequently used in biomedical applications because of their excellent biocompatibility [14,15]. However, polyurethanes are known to emit auto-fluorescence [16]. Be--cause the commercially available immuno-magnetic beads (Dynabeads Epithelial Enrich) are coated with polyurethane emitting auto-fluorescence, these beads cannot be used in our cellular analysis. The beads prepared by us exhibited very low auto-fluorescence because the surfaces of our immuno-magnetic beads are coated with a poly-glycidyl methacrylate layer that does not emit auto-fluorescence.

In the simulation study, our newly developed immuno-magnetic beads could retrieve EpCAM-positive cells efficiently. Moreover, the beads could isolate the endometrial cells from various types of cell adsorbed to a tampon. Both endometrial cancer cells and normal endometrial cells were EpCAM-positive. Almost EpCAM-positive cells from non-malignant controls were exfoliated normal endometrial cells. Meanwhile, EpCAM-positive cells from endometrial cancers were consisted of endometrial cancer cells and normal endometrial cells. Not only endometrial cancer cells but also tubal cancer, cervical cancer, or vaginal cancer cells may be exfoliated into a vaginal discharge. There is, therefore, potential to detect these cells in a same sample. In this study, magnetic beads conjugated with anti-human EpCAM mAb (EpCAM-beads) were used for isolation of exfoliated endometrial cancer cells from vaginal discharge. Since exfoliated cancer cells from squamous cell carcinoma (most of cervical cancer and vaginal cancer) are EpCAM-negative, they were not isolated by EpCAM-beads. On the other hand, exfoliated cancer cells from adenocarcinoma (most of tubal cancer and a few of cervical cancer) were isolated by EpCAM-beads because they were EpCAM-positive. Unfortunately, we do not have a mAb which can distinguish cervical cancer cells from normal squamous cells. In our previous study, most tampon-retrieved cells were granulocytes and normal squamous cells [12] and the rate of endometrial cells in menstrual blood was only 3% in this study. In particular, few endometrial cells were obtained from among tampon-retrieved cells of the non-malignant control in a non-menstrual period. The major symptom of endometrial cancer is abnormal uterine bleeding; thus, subjects with abnormal uterine bleeding or normal menstrual blood were enrolled in this clinical study as controls. A lot of EpCAM-positive endometrial cells were obtained from controls with menstrual period but the least EpCAM-positive cells were obtained from controls with non-menstrual period. Thus, menstrual blood was used for non-malignant control in this study. The median EpCAM-positive cells of controls were over 100. Meanwhile, major symptom of endometrial cancer patient was abnormal uterine bleeding. However, almost patients with endometrial cancer were in menopause and their endometria had changed to be atrophic. Therefore, a few exfoliated EpCAM-positive cells were obtained from patients with endometrial cancer but most of them appeared to be malignant endometrial cells. Immunomagnetic beads that could retrieve the endometrial cells from a sample of uterine blood appeared to be useful.

In this study, the detecting mAbs were the same as in our previous study [12]. Recently, several mAbs against EpCAM, EphA2, MMP2, survivin, and podoplanin were

investigated for endometrial cancer treatment and the detection of lymphovascular invasion [15,17-19]. However, these mAbs insufficient to detect endometrial cancer cells, so further development of endometrial cancer-specific mAbs should be performed. Meanwhile, several microRNAs (miRNAs) that were highly expressed in endometrial cancer tissue were reported [20-22]. The miRNA expression test of exfoliated endometrial cells might become an alternative endometrial cancer screening method in the future.

The present study showed that the sensitivity to detect endometrial cancer patients and the specificity for non-malignant controls with flow cytometry analysis were 73% and 75%, respectively. Meanwhile, the sensitivity and the specificity by imaging cytometry analysis were 46% and 81%, respectively. Generally, cancer screening is performed for average-risk population to reduce the cancer mortality in the group. Thus, cancer screening is performed annually and should be low-cost and non-(less)-invasive. Although sufficient sensitivity of cancer screening is 50% to 75%, specificity is needed over 95%. In this context, we have to admit that specificity of our cellular analysis was low. We are, therefore, developing further specific mAbs to increase the specificity. Recently serum human epididymis protein 4 (HE4) has been used for the detection of endometrial cancer [23-27]. Angioli et al. reported that the sensitivity and specificity of serum HE4 test were 59% and 100%, respectively [27]. Serum (plasma) protein analyses (containing HE4, CEA or CA125) were useful for detection of cancer relapse or therapeutic effect of chemotherapy. Therefore, these are used for so-called tumor markers as other cancers. For example, in colorectal cancer, CEA is useless for the early stage but is available as a tumor marker because serum CEA level in patients with early stage of colorectal cancer is not higher than that in healthy controls. Therefore, fecal occult blood test is generally used in colorectal cancer screening. With the same reason, serum protein was not useful for endometrial cancer screening and proteins derived from endometrial cancer cells were contained more in a vaginal discharge. It is then speculated that the vaginal discharge containing exfoliated cells is useful for endometrial cancer screening. These findings are still insufficient for endometrial cancer screening, so further investigations are needed.

Sensitivity and specificity of our cellular analysis are less than those of traditional methods, such as curettage. Histological diagnosis using endometrial cytology or biopsy is used for final diagnosis. However, examinees suffer physical and psychological pain with curettage. In addition, current screening methods including curettage are time consuming and expensive and the medical examination is inconvenient for women. Our novel cyto-

logical or histological methods are non-invasive compared to former cytology or histology. Cellualr analysis using immuno-magnetic beads and fluorostaining could be performed without human's eye; thus, it could reduce the cost. Moreover, the procedures of cellular analysis can be performed automatically using immuno-magnetic beads and magnet. In this method, the women only collect vaginal discharge using a tampon and send the sample to a laboratory at suitable storage condition. Although both the sensitivity and specificity should be enhanced, we think that this method may become convenient and cheap, and the new mAbs sets detecting endometrial cancer should be developed. In this study, the number of clinical samples was small. Thus, many issues remain to be resolved in order to improve these cellular analyses for the detection of endometrial cancer cells using immuno-magnetic beads and flow cytometry. Our immuno-magnetic beads have very low auto-fluorescence, so they should be useful for fluorescent analysis, such as fluorescent immunochemical staining. In the future, these novel materials could lead to the next-generation methodology for cellular diagnosis.

5. Acknowledgements

REFERENCES

[1] F. Amant, P. Moerman, P. Neven, D. Timmerman, E. Van Limbergen and I. Vergote, "Endometrial Cancer," *Lancet*, Vol. 366, No. 9484, 2005, pp. 491-505. http://dx.doi.org/10.1016/S0140-6736(05)67063-8

[2] R. Siegel, D. Naishadham and A. Jemal, "Cancer Statistics, 2013," *CA: A Cancer Journal for Clinicians*, Vol. 63, No. 1, 2013, pp. 11-30. http://dx.doi.org/10.3322/caac.21166

[3] T. Matsuda, T. Marugame, K. Kamo, K. Katanoda, W. Ajiki, T. Sobue and Group Japan Cancer Surveillance Research, "Cancer Incidence and Incidence Rates in Japan in 2006: Based on Data from 15 Population-Based Cancer Registries in the Monitoring of Cancer Incidence in Japan (MCIJ) Project," *Japanese Journal of Clinical Oncology*, Vol. 42, No. 2, 2012, pp. 139-147. http://dx.doi.org/10.1093/jjco/hyr184

[4] R. A. Smith, D. Brooks, V. Cokkinides, D. Saslow and O. W. Brawley, "Cancer Screening in the United States, 2013: A Review of Current American Cancer Society Guidelines, Current Issues in Cancer Screening, and New Guidance on Cervical Cancer Screening and Lung Cancer Screening," *CA: A Cancer Journal for Clinicians*, Vol. 63, No. 2, 2013, pp. 88-105. http://dx.doi.org/10.3322/caac.21174

[5] R. A. Smith, V. Cokkinides and O. W. Brawley, "Cancer Screening in the United States, 2009: A Review of Current American Cancer Society Guidelines and Issues in Cancer Screening," *CA: A Cancer Journal for Clinicians*, Vol. 59, No. 1, 2009, pp. 27-41. http://dx.doi.org/10.3322/caac.20008

[6] J. Holst, O. Koskela and B. von Schoultz, "Endometrial Findings Following Curettage in 2018 Women According to Age and Indications," *Annales Chirurgiae et Gynaecologiae*, Vol. 72, No. 5, 1983, pp. 274-277.

[7] T. Gredmark, S. Kvint, G. Havel and L. A. Mattsson, "Histopathological Findings in Women with Postmenopausal Bleeding," *British Journal of Obstetrics and Gynaecology*, Vol. 102, No. 2, 1995, pp. 133-136. http://dx.doi.org/10.1111/j.1471-0528.1995.tb09066.x

[8] Y. C. Choo, K. C. Mak, C. Hsu, T. S. Wong and H. K. Ma, "Postmenopausal Uterine Bleeding of Nonorganic Cause," *Obstetrics and Gynecology*, Vol. 66, No. 2, 1985, pp. 225-228.

[9] B. Gull, B. Karlsson, I. Milsom and S. Granberg, "Can Ultrasound Replace Dilation and Curettage? A Longitudinal Evaluation of Postmenopausal Bleeding and Transvaginal Sonographic Measurement of the Endometrium as Predictors of Endometrial Cancer," *American Journal of Obstetrics and Gynecology*, Vol. 188, No. 2, 2003, pp. 401-408.

[10] E. Kondo, T. Tabata, Y. Koduka, K. Nishiura, K. Tanida, T. Okugawa and N. Sagawa, "What Is the Best Method of Detecting Endometrial Cancer in Outpatients? Endometrial Sampling, Suction Curettage, Endometrial Cytology," *Cytopathology*, Vol. 19, No. 1, 2008, pp. 28-33. http://dx.doi.org/10.1111/j.1365-2303.2007.00509.x

[11] B. R. Kipp, F. Medeiros, M. B. Campion, T. J. Distad, L. M. Peterson, G. L. Keeney, K. C. Halling and A. C. Clayton, "Direct Uterine Sampling with the Tao Brush Sampler Using a Liquid-Based Preparation Method for the Detection of Endometrial Cancer and Atypical Hyperplasia: A Feasibility Study," *Cancer*, Vol. 114, No. 4, 2008, pp. 228-235. http://dx.doi.org/10.1002/cncr.23636

[12] Y. Koga, M. Yasunaga, M. Kajikawa, E. Shimizu, R. Takamatsu, R. Kataoka, Y. Murase, Y. Sasajima, T. Kasamatsu, T. Kato, T. Onda, S. Ikeda, M. Ishikawa, K. Ishitani, H. Ohta and Y. Matsumura, "Novel Virtual Cytological Analysis for the Detection of Endometrial Can-

cer Cells Using Autoscan Fluoromicroscopy," *Cancer Science*, Vol. 102, No. 5, 2011, pp. 1068-1075.
http://dx.doi.org/10.1111/j.1349-7006.2011.01903.x

[13] Y. Koga, M. Yasunaga, S. Katayose, Y. Moriya, T. Akasu, S. Fujita, S. Yamamoto, H. Baba and Y. Matsumura, "Improved Recovery of Exfoliated Colonocytes from Feces Using Newly Developed Immunomagnetic Beads," *Gastroenterology Research & Practice*, Vol. 2008, 2008, Article ID: 605273.
http://dx.doi.org/10.1155/2008/605273

[14] S. Grenier, M. Sandig, D. W. Holdsworth and K. Mequanint, "Interactions of Coronary Artery Smooth Muscle Cells with 3D Porous Polyurethane Scaffolds," *Journal of Biomedical Materials Research Part A*, Vol. 89, No. 2, 2009, pp. 293-303. http://dx.doi.org/10.1002/jbm.a.31972

[15] W. M. Merritt, A. A. Kamat, J. Y. Hwang, J. Bottsford-Miller, C. Lu, Y. G. Lin, D. Coffey, W. A. Spannuth, E. Nugent, L. Y. Han, C. N. Landen, A. M. Nick, R. L. Stone, K. Coffman, E. Bruckheimer, R. R. Broaddus, D. M. Gershenson, R. L. Coleman and A. K. Sood, "Clinical and Biological Impact of EphA2 Overexpression and Angiogenesis in Endometrial Cancer," *Cancer Biological Therapy*, Vol. 10, No. 12, 2010, pp. 1306-1314.
http://dx.doi.org/10.4161/cbt.10.12.13582

[16] S.-K. Wang and C. S. P. Sung, "Spectroscopic Characterization of Model Urea, Urethane Compound, and Diamine Extender for Polyurethane-Urea," *Macromolecules*, Vol. 35, No. 3, 2002, pp. 877-882.
http://dx.doi.org/10.1021/ma011316+

[17] K. El-Sahwi, S. Bellone, E. Cocco, F. Casagrande, M. Bellone, M. Abu-Khalaf, N. Buza, F. A. Tavassoli, P. Hui, D. Ruttinger, D. A. Silasi, M. Azodi, P. E. Schwartz, T. J. Rutherford, S. Pecorelli and A. D. Santin, "Overexpression of EpCAM in Uterine Serous Papillary Carcinoma: Implications for EpCAM-Specific Immunotherapy with Human Monoclonal Antibody Adecatumumab (MT201)," *Molecular Cancer Therapy*, Vol. 9, No. 1, 2010, pp. 57-66. http://dx.doi.org/10.1158/1535-7163.MCT-09-0675

[18] E. Yilmaz, M. Koyuncuoglu, I. B. Gorken, E. Okyay, B. Saatli, E. C. Ulukus and U. Saygili, "Expression of Matrix Metalloproteinase-2 and Survivin in Endometrioid and Nonendometrioid Endometrial Cancers and Clinicopathologic Significance," *Journal of Gynecologic Oncology*, Vol. 22, No. 2, 2011, pp. 89-96.
http://dx.doi.org/10.3802/jgo.2011.22.2.89

[19] S. K. Weber, A. Sauerwald, M. Polcher, M. Braun, M. Debald, N. B. Serce, W. Kuhn, G. Brunagel-Walgenbach and C. Rudlowski, "Detection of Lymphovascular Invasion by D2-40 (Podoplanin) Immunoexpression in Endometrial Cancer," *International Journal of Gynecological Cancer*, Vol. 22, No. 8, 2012, pp. 1442-1448.
http://dx.doi.org/10.1097/IGC.0b013e318269139b

[20] T. Boren, Y. Xiong, A. Hakam, R. Wenham, S. Apte, Z.

Wei, S. Kamath, D. T. Chen, H. Dressman and J. M. Lancaster, "MicroRNAs and Their Target Messenger RNAs Associated with Endometrial Carcinogenesis," *Gynecologic Oncology*, Vol. 110, No. 2, 2008, pp. 206-215.
http://dx.doi.org/10.1016/j.ygyno.2008.03.023

[21] W. Wu, Z. Lin, Z. Zhuang and X. Liang, "Expression Profile of Mammalian microRNAs in Endometrioid Adenocarcinoma," *European Journal of Cancer Prevention*, Vol. 18, No. 1, 2009, pp. 50-55.
http://dx.doi.org/10.1097/CEJ.0b013e328305a07a

[22] T. K. Chung, T. H. Cheung, N. Y. Huen, K. W. Wong, K. W. Lo, S. F. Yim, N. S. Siu, Y. M. Wong, P. T. Tsang, M. W. Pang, M. Y. Yu, K. F. To, S. C. Mok, V. W. Wang, C. Li, A. Y. Cheung, G. Doran, M. J. Birrer, D. I. Smith and Y. F. Wong, "Dysregulated Micrornas and Their Predicted Targets Associated with Endometrioid Endometrial Adenocarcinoma in Hong Kong Women," *International Journal of Cancer*, Vol. 124, No. 6, 2009, pp. 1358-1365.
http://dx.doi.org/10.1002/ijc.24071

[23] E. Bignotti, M. Ragnoli, L. Zanotti, S. Calza, M. Falchetti, S. Lonardi, S. Bergamelli, E. Bandiera, R. A. Tassi, C. Romani, P. Todeschini, F. E. Odicino, F. Facchetti, S. Pecorelli and A. Ravaggi, "Diagnostic and Prognostic Impact of Serum HE4 Detection in Endometrial Carcinoma Patients," *British Journal of Cancer*, Vol. 104, No. 9, 2011, pp. 1418-1425.
http://dx.doi.org/10.1038/bjc.2011.109

[24] E. Kalogera, N. Scholler, C. Powless, A. Weaver, R. Drapkin, J. Li, S. W. Jiang, K. Podratz, N. Urban and S. C. Dowdy, "Correlation of Serum HE4 with Tumor Size and Myometrial Invasion In Endometrial Cancer," *Gynecologic Oncology*, Vol. 124, No. 2, 2012, pp. 270-275.
http://dx.doi.org/10.1016/j.ygyno.2011.10.025

[25] I. Mutz-Dehbalaie, D. Egle, S. Fessler, M. Hubalek, H. Fiegl, C. Marth and A. Widschwendter, "HE4 Is an Independent Prognostic Marker in Endometrial Cancer Patients," *Gynecologic Oncology*, Vol. 126, No. 2, 2012, pp. 186-191. http://dx.doi.org/10.1016/j.ygyno.2012.04.022

[26] R. G. Moore, C. M. Miller, A. K. Brown, K. Robison, M. Steinhoff and G. Lambert-Messerlian, "Utility of Tumor Marker HE4 to Predict Depth of Myometrial Invasion in Endometrioid Adenocarcinoma of the Uterus," *International Journal of Gynecological Cancer*, Vol. 21, No. 7, 2011, pp. 1185-1190.
http://dx.doi.org/10.1097/IGC.0b013e3182229ad8

[27] R. Angioli, F. Plotti, S. Capriglione, R. Montera, P. Damiani, R. Ricciardi, A. Aloisi, D. Luvero, E. V. Cafa, N. Dugo, M. Angelucci and P. Benedetti-Panici, "The Role of Novel Biomarker HE4 in Endometrial Cancer: A Case Control Prospective Study," *Tumour Biology*, Vol. 34, No. 1, 2013, pp. 571-576.
http://dx.doi.org/10.1007/s13277-012-0583-0

Original article

Sentinel and nonsentinel lymph node assessment using a combination of one-step nucleic acid amplification and conventional histological examination

CrossMark

Kenjiro Jimbo [a,*], Takayuki Kinoshita [a], Junko Suzuki [a], Sota Asaga [a], Takashi Hojo [a], Masayuki Yoshida [b], Hitoshi Tsuda [b]

[a] Breast Surgery Division, National Cancer Center Hospital, Tokyo, Japan
[b] Department of Pathology and Clinical Laboratories, National Cancer Center Hospital, Tokyo, Japan

ARTICLE INFO

ABSTRACT

Background: Clinical significance of intraoperative sentinel lymph node (SLN) metastases detection using one-step nucleic acid amplification (OSNA) has not been thoroughly investigated. The aim of this study was to assess the usefulness of using a combination of OSNA and conventional histological examinations. Materials and methods: We included 772 consecutive patients with clinical node-negative cTis-cT3 primary breast cancer who underwent SLN biopsy with intraoperative OSNA and multi-section histological examination at our institution. We estimated the concordance rate and compared SLN metastases detection rates between the two methods. We also compared non-SLN metastasis detection rate between patients who tested positive in OSNA and those who tested positive in histology.
Results: Among 772 patients, SLN metastases were intraoperatively detected in 211 (26.4%) by either OSNA or histology, in 168 (21.8%) by OSNA, and in 150 (19.4%) by histology. The concordance rate between OSNA and histological examination was 89.2%, but only 123 (58.8%) patients tested positive in both OSNA and histology; 45 were positive in OSNA only and 43 were positive in histology only.
SLN status as per both OSNA and histology was significantly correlated with the presence of non-SLN metastases and multivariate analysis-identified independent predictive factors of non-SLN metastases.
Conclusions: Intraoperative SLN metastases detection may be more accurate with a combination of OSNA and histological examination than with OSNA or histological examination alone. By using both methods, we can reduce the risk of false negative rate in SLN biopsy, and may prevent physicians from overlooking patients with non-SLN metastases.

Introduction

Conventional intraoperative histological examinations in sentinel lymph node (SLN) biopsy are well known to show high (10–30%) false-negative results for metastatic foci because only a few thin sections from a lymph node are examined in this technique. The suboptimal quality of frozen section slides and oversights by pathologists increase the false-negative detection rate. Moreover, use of more intensive methods, such as serial-step section examination of each SLN, is impractical because it requires a heavy workload for pathologists [1].

Molecular assays have been developed to overcome these shortcomings. The one-step nucleic acid amplification (OSNA) assay (Sysmex, Kobe, Japan), which involves amplification and quantitative measurement of cytokeratin 19 (CK19) mRNA levels, can detect lymph node metastases as accurately as can conventional histological examination, is faster [2], and detects more low-volume tumor nodal involvement than do conventional histological methods. However, whether these techniques can verify the need for further axillary treatment is unclear [3].

This study compared detection rates between OSNA and histological examination, both for intraoperative SLN metastases and for non-SLN metastases. We also discuss the possibility of omitting axillary lymph node dissection (ALND) for some patients with positive SLN metastases (SLN+)—specifically, those histological micrometastases or isolated tumor cells (ITC), and OSNA 1+ patients.

Materials and methods

Subjects comprised 772 consecutive patients with clinically node-negative Tis-T3 primary breast cancer who underwent SLN

* Corresponding author. Tel.: +81 3 3542 2511; fax: +81 3 3542 3815.
E-mail address: kjimbo@ncc.go.jp (K. Jimbo).

biopsy with combined intraoperative OSNA and histological examination between February 2010 and June 2012 at the National Cancer Center Hospital, Tokyo, Japan. Patients who received neoadjuvant therapy, and male patients were excluded.

Clinical and pathological T and N factors were based on the Cancer Staging Manual of the American Joint Committee on Cancer (AJCC), 7th edition [4]. Patient characteristics are listed in Table 3. The cut-off value for ER and PR positivity was 10% positive cells for both, irrespective of intensity. HER2 positivity was defined as an HER2 score of >3 (>30% strong membrane immunoreaction-positive cells) or an HER2 gene/centromere 17 ratio of ≥ 2.0 as assessed by fluorescence in situ hybridization.

SLN biopsy procedure

First, 0.1 ml of 99mTc-phytate was prepared. Half of this solution was injected into the dermis of the areola while the remainder was injected into the dermis over the tumor on the day before surgery. In all patients, lymphoscintigraphy was performed 3 h after injection. In addition, 3–4 ml blue dye or 1 ml indocyanine green was injected into the peritumoral space or areola at the time of surgery. SLNs were identified using a hand-held gamma probe guided by nodal staining. Nodes that responded to near-infrared light, were stained with blue dye, or had high radioactive count were considered as SLNs. No more than four resected SLNs per patient were intraoperatively evaluated by both OSNA and histological examination. We omitted axillary dissection in patients with no SLN metastases and performed axillary dissection in patients with histological macrometastases, micro-metastases, or ITCs in SLNs or positivity in OSNA. These patients were considered SLN$^+$ in this study.

Preparation of SLNs

Excised SLNs were cut into 2-mm slices along the short axis and were alternately prepared for OSNA and histological examination.

Histological examination of SLNs

The sliced tissue specimens for histological examination were first subjected to intraoperative frozen-section diagnosis. These sliced tissues were then fixed in 10% formalin overnight, embedded in paraffin, cut into 4-μm-thick sections, stained with hematoxylin and eosin (HE), and subjected to permanent-section diagnosis.

Macrometastases were defined as SLN$^+$ that measured >2 mm in greatest diameter, micrometastases as SLN$^+$ that measured 0.2–2 mm in greatest diameter, and ITC as small clusters of cells ≤ 0.2 mm across their greatest diameter, as detected by HE staining or immunohistochemistry. Although ITCs are recommended to be classified as pN0(i$^+$), they were considered as metastases in the present study.

OSNA assay for SLN examination

The details of the OSNA assay based on the RT-LAMP method were previously described by Tsujimoto et al. [5] Briefly, resected SLNs were homogenized with 4 ml lysis buffer solution and centrifuged at 10000× g at room temperature. The RD-100i system (Sysmex, Kobe, Japan) was used to analyze 2 μl of the lysed SLN supernatant.

Using OSNA, SLNs were considered to be SLN$^-$ when the CK19 mRNA copy number was $<2.5 \times 10^2/\mu l$, SLN$^+$ 1$^+$ when the copy number was $2.5 \times 10^2/\mu l$–$5.0 \times 10^3/\mu l$, and metastases-positive 2$^+$ when the copy number was $>5.0 \times 10^3/\mu l$. A 1:10 dilution of homogenized lymph node solution was always prepared for each patient and analyzed simultaneously because excess protein may

interfere with the RT-LAMP reaction [5]. Lymph node lysates showing >250 copies/μl of CK19 mRNA only in the 1:10 diluted solution were classified as positive and designated as +I (inhibition positive). Permanent histological tissue sections were immunostained for CK19 when samples that were SLN$^-$ by OSNA were histologically SLN$^+$.

Permanent histological examination of non-SLNs

ALND was performed when specimens were SLN$^+$ by either OSNA or histology. All non-SLNs were bisected along the long axis after formalin fixation. For each non-SLN, only one permanent HE tissue section for the representative cut surface was histologically examined.

Statistical analysis

We used the Mann–Whitney test to compare age and BMI between SLN$^+$ and SLN$^-$ patients, the χ^2 test to compare other variables, and performed logistic regression analysis to investigate odds ratios of individual parameters for non-SLN metastases. $P < 0.05$ was considered statistically significant. Confidence intervals (CIs) were set at the 95% level. SPSS statistical software (version 19, IBM SPSS Statistics, Chicago, IL, USA) was used for all statistical analyses.

Results

Concordance rate between histology and OSNA

SLN metastases, including ITC, were detected in 211 (27.3%) of the 772 patients: 145 (18.8%) by intraoperative examination of frozen HE-stained sections, 168 (21.8%) by OSNA, and 166 (21.5%) by the examination of permanent HE-stained sections (Table 1). Because we regarded ITC as histological metastases, ALND was performed for patients with ITC in SLNs.

The concordance rate between OSNA and intraoperative histological diagnosis was 88.2%, and that between OSNA and permanent histological diagnosis was 88.6%. The kappa value between OSNA diagnosis and permanent histological diagnosis was 0.66, indicating substantial concordance.

Table 1
Concordance of sentinel lymph node metastasis between OSNA diagnosis and histological diagnosis.

A. Comparison with frozen section diagnosis			
	Number of patients (%)		
	Total	Intraoperative frozen section	
		Histology (+)	Histology (−)
OSNA (+)	168	111	57
OSNA (−)	604	34	570
Total	772	145	627

B. Comparison with frozen section + permanent section diagnosis			
	Number of patients (%)		
	Total	Intraoperative + permanent sections	
		Histology (+)	Histology (−)
OSNA (+)	168	123	45
OSNA (−)	604	43	561
Total κ = 0.66	772	166	606

Histology (+) includes macrometastasis, micrometastasis, and isolated tumor cells (ITC), whereas Histology (−) includes others. OSNA (−) includes OSNA 2+, 1+, and +I, whereas OSNA (−) includes OSNA-.

Table 2
Detailed comparison of OSNA results with histological results for sentinel lymph node metastasis.

OSNA	Number of cases (%)				
	Total	Histological diagnosis (permanent section)			
		Macromestasitasis	Micrometastasis	ITC	Negative
2+	90	78 (87)	8 (9)	0 (0)	4 (4)
1+	72	16 (22)	15 (21)	5 (7)	36 (50)
+I	6	1 (17)	0 (0)	0 (0)	5 (83)
−	604	9 (1)	23 (4)	11 (2)	561 (93)
Total	772	104	46	16	606

Among the 168 OSNA$^+$ patients, SLN metastases were histologically detected in 123 (73%), including five with ITC. The remaining 45 (27%) patients were histologically SLN$^-$ (Tables 1 and 2). When OSNA results were stratified, SLN$^+$ rate per permanent histological examination was 96% (86 of 90) for OSNA 2 + patients, 50% (36 of 72) for OSNA 1 + patients, and 17% (one of six) for OSNA + I patients. Among the 604 OSNA$^-$ patients, 43 (7%) were histologically SLN$^+$.

In contrast, 123 (74%) of the 166 histologically SLN$^+$ patients, including 16 with ITC in SLNs, were SLN$^+$ using OSNA.

Clinicopathological correlation with SLN status by histology and OSNA

Clinicopathological characteristics of the 772 patients are listed in Table 3. For SLN statuses detected by both permanent histology and OSNA, SLN metastases significantly correlated with cT-factor, pT-factor, histological type, LVI (lymphovascular invasion) and histological grade.

There were no significant differences in characteristics between patients with SLN metastases detected by OSNA and histological

Table 3
Correlations of clinicopathological parameters with sentinel lymph node status, detected by histopathological examination and by OSNA method.

Parameter	Number of cases (%)						
	Total N = 772	SLN status (%)			SLN status (%)		
		Histology (+)N = 166	Histology (−)N = 606	p	OSNA (+)N = 168	OSNA (−)N = 604	p
Age							
Average (range)	56.3 (27–92)	54.9 (27–84)	56.8 (28–92)	NS	54.1 (27–92)	56.9 (28–92)	NS
<50	256	59 (23)	197 (77)		64 (25)	191 (75)	
≧50	516	107 (21)	409 (79)		104 (20)	413 (80)	
Menopause							
Premenopausal	311	72 (23)	239 (77)	NS	78 (25)	233 (75)	NS
Postmenopausal	457	94 (21)	363 (79)		90 (20)	367 (80)	
Unknown	4	0	4 (100)		0	4 (100)	
BMI							
Average (range)	22.1 (13.2–40)	22.6 (17–40)	22.0 (13.2–35.8)	NS	22.1 (17–40)	22.1 (13.2–35.8)	NS
<25	645	138 (21)	507 (79)		147 (23)	498 (77)	
≧25	126	28 (22)	98 (78)		21 (17)	105 (83)	
Unknown	1	0 (0)	1 (100)		0 (0)	1 (100)	
CT-factor							
Tis	159	6 (4)	153 (96)	<0.0001	8(5)	151 (95)	<0.0001
T1	355	66 (19)	289 (81)		76 (21)	279 (79)	
T2	252	90 (36)	162 (64)		80 (32)	172 (68)	
T3	6	4 (67)	2 (33)		4 (67)	2 (33)	
PT-factor							
Tis	119	0 (0)	119 (100)	<0.0001	8 (7)	111 (93)	<0.0001
T1	413	72 (17)	341 (83)		73 (18)	340 (82)	
T2	209	73 (35)	136 (65)		68 (33)	141 (67)	
T3	29	21 (72)	8 (28)		19 (66)	10 (34)	
Unknown	2	0 (0)	2 (100)		0 (0)	2 (100)	
His to logical type							
Carcinoma in situ	119	0 (0)	119 (100)	<0.0001	8 (7)	111 (93)	<0.0001
Invasive ductal	566	150 (27)	416 (73)		143 (25)	423 (75)	
Special	86	16 (19)	70 (21)		17 (20)	69 (80)	
Others	1	0	1 (100)		0 (0)	1 (100)	
Lymphovascular invasion							
Negative	533	65 (12)	468 (88)	<0.0001	74 (14)	459 (86)	<0.0001
Positive	230	101 (44)	129 (56)		92 (40)	138 (60)	
Unknown	9	0 (0)	9 (100)		2 (22)	7 (78)	
Histological grade							
1	217	17 (8)	200 (92)	<0.0001	26(12)	191 (88)	<0.0001
2	351	95 (27)	256 (73)		84 (24)	267 (76)	
3	202	54 (27)	148 (73)		58 (29)	144 (71)	
Unknown	2	0 (0)	2 (100)		0	2 (100)	
Hormone receptor							
Negative	113	19 (17)	94 (83)	NS	21 (19)	92 (81)	NS
Positive	658	146 (22)	512 (78)		146 (22)	512 (78)	
Unknown	1	1 (100)	0 (0)		1 (100)	0 (0)	
HER2							
Negative	671	148 (22)	523 (78)	NS	147 (22)	524 (88)	NS
Positive	86	17 (20)	69 (80)		18 (21)	68 (89)	
Unknown	15	1 (7)	14 (93)		3 (20)	12 (80)	

Histology (+) includes macrometastasis, micrometastaas, and isolated tumor cells (ITC), whereas Histology (−) includes others. OSNA (+) includes OSNA 2+, 1+, and +I, whereas OSNA (−) includes OSNA−.

method. However, despite no statistical significance, percentages of early and low-grade tumors tended to be larger in the former group: no patient with carcinoma in situ showed histological SLN metastases, whereas eight (7%) of 119 patients with carcinoma in situ showed positivity in OSNA. Similarly, LVI⁻ (14% vs 12%), and histological grade 1 (12% vs 8%) tumors tended to test positive more frequently in OSNA (Table 3).

Correlation of SLN status with non-SLN status in patients who underwent ALND

Among the 211 SLN⁺ patients, 206 underwent ALND after SLN biopsy. The correlation of SLN status with non-SLN status based on OSNA and permanent histological examination is summarized in Table 4.

Among the 206 SLN⁺ by OSNA or histology, 53 (26%) had non-SLN metastases. The overall incidence of non-SLN metastases among patients with histological SLN metastases was 32% (52 of 162): 40% (42 of 104), 20% (nine of 44), and 8% (one of 13) for patients with macrometastases, micrometastases, and ITC in SLNs, respectively. In contrast, only one (2%) of the 44 patients with OSNA⁺ but histology⁻ SLN metastases exhibited non-SLN metastases (Table 4).

Clinicopathological characteristics were analyzed in a multivariate logistic regression model. Histological SLN status (macrometastases/nonmalignant cells: odds ratio, 12.17; 95% confidence interval (CI); 1.45–102.34; $P = 0.020$) and OSNA-determined SLN status (OSNA2⁺ to OSNA–: odds ratio, 4.75; 95% CI, 1.23–17.35; $P = 0.018$) were identified as independent predictive factors for non-SLN metastases (Table 5). These data indicate that OSNA 1⁺ status was not an independent predictor for non-SLN metastases.

Discussion

The concordance rate of SLN metastasis detection between OSNA and histological diagnoses is reportedly high, ranging from 86.3% to 96.3% [1,2,7–14]. The SLN metastasis detection rate by OSNA was higher than that by histological examination because OSNA can detect tumor cells in whole tissues [14–16].

Table 4
Comparison between sentinel lymph node (SLN) status and non-SLN status.

SLN status			Number of cases (%)			
			Total	Non-SLN metastases		
pN stage	Histology	OSNA		Positive	Negative	Subtotal
PN1	Macrometastasis	2+	78	37 (47)	41	42/104 (40)
		1+	16	4 (25)	12	
		+I	1	0 (0)	1	
		–	9	1 (11)	8	
PN1mi	Micrometastasis	2+	8	1 (13)	7	9/45 (20)
		1+	15	5 (33)	10	
		–	22	3 (14)	19	
pN0(i+)ª	ITC	2+	0	0 (0)	0	1/13 (8)
		1+	5	1 (20)	4	
		–	8	0 (0)	8	
pN0 (mol+)ᵇ	–	2+	4	1 (25)	3	1/44 (2)
		1+	35	0 (0)	35	
		+I	5	0 (0)	5	
			206	53	154	53/206 (26)

Five patients who did not receive ALND were excluded from the calculation.
ª Axillary macro- or micrometastases absent but ITC present as per histology, regardless of OSNA results.
ᵇ Axillary metastases absent as per histology but present as per OSNA (2+, 1+, and/or + I).

Table 5
Predictive factors for non-SLN metastasis by multivariate logistic regression model analysis.

Parameter	Odds Ratio	95% confidence interval	p Value
pT factor			
PT1	1		
pT2	1.29	0.59–2.83	0.52
pT3	2.64	0.89–7.85	0.081
Hormone receptor status			
Positive	1		
Negative	2.47	0.88–6.96	0.088
SLN status by histology			
No malignant cell	1		
ITC	4.99	0.26–95.17	0.285
Micrometastasis	8.98	0.99–81.76	0.052
Macrometastasis	12.17	1.45–102.34	0.02
SLN status by OSNA			
–	1		
1+	2.27	0.59–8.66	0.232
2+	4.75	1.23–17.35	0.018

We did not include patients with pTis and OSNA + I in the analysis because there were no patients with non-SLN metastases in these groups.

However, histological corroboration of cancer volume is impossible if entire SLN tissues are used for OSNA assays. We considered that comparison of intraoperative OSNA results with intraoperative histology results was necessary for several patients before complete substitution of intraoperative histological diagnosis by OSNA. In this study, the SLN metastasis detection rate using combined OSNA and histology was 27.1% higher than that by histology only and 25.6% higher than that by OSNA only.

Among the SLN⁺ 211 patients using either method, 88 showed discordant results. Only 123 (58.3%) patients were both OSNA⁺ and histology⁺. Such discordances were especially common among patients who were OSNA 1⁺ (50%, 36 of 72), OSNA + I (83%, five of six), and those with histology⁺ micrometastases (50%, 23 of 46) and histology⁺ ITC (69%, 11 of 16) in SLNs. In contrast, the discordance rate was only 4% (four of 90) among OSNA 2⁺ patients and 9% (nine of 104) among patients with histology⁺ macrometastases.

Reportedly, most discrepancies occur because of uneven distribution of minuscule metastases [6,7]. Vegue et al. showed that histological examination of a single SLN section misclassified 41.8% patients as SLN⁻ compared OSNA data ($P = 0.007$) [17]. Although we histologically assessed multiple slices of SLN samples (2-mm intervals, two to seven slices per node) to ensure accurate comparison of SLN⁺ rates between the two methods, uneven distribution of metastatic foci in SLNs appeared to occur in >40% SLN⁺ patients. Tamaki et al. examined SLN metastases using both OSNA and histology methods similar to those used in the present study and reported that discordant results due to uneven distribution occurred in 38% of patients with OSNA⁺ SLNs and 11% of patients with histology⁺ SLNs [7].

Another possible explanation for this discordance may lie in the false-negative results exhibited by tumors with low CK19 expression. Low CK19 protein expression is reported in approximately 2–3% of breast cancers [6,18]. In the present study, we performed CK19 immunostaining for 16 of 31 patients with histology⁺ but OSNA⁻ tumors; however, we found that only one of 16 patients with positive residual SLN metastases was CK19⁻. Therefore, most discordant results were attributed to uneven distribution of tumor cell foci in each SLN.

In the present study, the non-SLN metastasis detection rate was high in OSNA 2⁺ patients (43%, 39 of 90) and patients with SLN micrometastases (40%, 42 of 104). In addition, the incidences of non-SLN metastases among OSNA 1⁺ patients and patients

with histology[+] micrometastases were 14% (10 of 71) and 20% (nine of 45), respectively. The present data concords with those reported by Castellano et al., in which OSNA 2[+] patients had a 42% chance of non-SLN metastases while OSNA 1[+] patients had a 22% chance of non-SLN metastases [6]. When both OSNA and histology were combined, the rate of non-SLN metastasis detection was extremely low in patients with histology[+] ITC in SLNs (regardless of OSNA status; 8%; 1 of 13), OSNA 1[+] patients without histological metastases (0%; 0 of 35), and OSNA + I patients without histological metastases (0%; 0 of five). Both histology[+] metastasis size and semiquantitative OSNA SLN data were significant independent predictors of non-SLN metastases according to logistic regression analysis. Moreover, combined use of OSNA and histological examination could identify patients whose SLN statuses, — specifically, ITC, OSNA 1[+], and OSNA + I, without histology[+] tumor deposits — , correlated with low risk of non-SLN metastasis.

Non-SLN metastases would have been overlooked in maximum 10% (four of 39) of SLN[−] patients if OSNA alone had been used. Similarly, non-SLN metastases would have been overlooked in 2% (one of 44) of SLN[−] patients if histological examination alone had been used. These estimations imply that ALND can be omitted in patients with SLN[+] detected by OSNA only in combined OSNA and histological examination. The non-SLN metastasis detection rate was much lower in histology[−] SLNs than for OSNA[−] SLNs when combined examination was used.

OSNA tended to detect SLN metastases more frequently than histological examination in primary tumors with non-invasive histology, histological grade 1, and lack of LVI. Although Osako et al. reported that OSNA could detect metastases more frequently than histological frozen-section examination in elderly or post-menopausal patients [15], we could not find such an interaction on using OSNA.

In the present study, there were 21 discordant diagnoses between intraoperative frozen section examination and permanent section examination. These included three cases of macro-metastases, 11 of micrometastases, and seven of ITC. OSNA detected more than half of the metastases missed by frozen section diagnosis: two of three cases of macrometastasis samples, six of 11 cases of micrometastasis, and four of seven cases of ITC samples. An advantage of using the OSNA assay is that it confirms histological results and identifies patients who require ALND. However, OSNA may also lead to unnecessary ALNDs. Given these circumstances, combining OSNA and histology can prevent physicians from overlooking SLN and non-SLN metastases that can be missed when either method is used alone.

ALND was recently shown to have no significant influence on clinical outcomes of patients with micrometastases or ITC [19,20]. Osako et al. showed that routine histological examination of non-SLN metastases could overlook many occult metastases that can be detected by combined OSNA and histological examination [21]. Our previous study found that SLN and non-SLN occult metastases that were not detected routinely but detected by serial-step sections at 85-μm intervals did not have significant prognostic implications [22].

The OSNA assay is a promising alternative or additional tool for intraoperative detection of SLN metastases. Because of the low rate of metastases to non-SLNs, ALND may be omitted in patients with OSNA 1[+]/histology[−] SLNs or OSNA[−]/histology[+] ITC[+] SLNs when OSNA and histological examination are combined.

To date, however, there is no evidence of whether or not metastases evaluated only by molecular analysis require ALND. Further data on tumor recurrence and patient survival will clarify how SLN metastases detected by molecular methods can be optimally managed.

Conclusions

Intraoperative SLN metastasis detection may be more accurate using a combination of OSNA and histological examination than with OSNA or histological examination alone. This combination technique may prevent physicians from overlooking patients with non-SLN metastases. Although stratification of non-SLN[+] and non-SLN[−] patients according to the present OSNA categories (2[+], 1[+], and +I) is not perfect, more complete predictions of non-SLN metastases using OSNA may only be possible if stratification of these categories is improved in the near future.

Role of funding source

Conflict of interest statement

Acknowledgments

References

[1] Tamaki Y, Akiyama F, Iwase T, Kaneko T, Tsuda H, Sato K, et al. Molecular detection of lymph node metastases in breast cancer patients: results of a multicenter trial using the one-step nucleic acid amplification assay. Clin Cancer Res 2009;15:2879–84.

[2] Sagara Y, Ohi Y, Matsukata A, Yotsumoto D, Baba S, Tamada S, et al. Clinical application of the one-step nucleic acid amplification method to detect sentinel lymph node metastases in breast cancer. Breast Cancer 2011. http://dx.doi.org/10.1007/s12282-011-0324-z.

[3] Cserni G. Intraoperative analysis of sentinel lymph nodes in breast cancer by one-step nucleic acid amplification. J Clin Pathol 2012;65:193–9.

[4] Edge SB, Byrd DR, Compton CC, Fritz AG, Greene FL, Trotti A. American joint committee on cancer cancer staging manual. 7th ed. New York, NY: Springer; 2010.

[5] Tsujimoto M, Nakabayashi K, Yoshidome K, Kaneko T, Iwase T, Akiyama F, et al. One-step nucleic acid amplification for intraoperative detection of lymph node metastasis in breast cancer patients. Clin Cancer Res 2007;13:4807–16.

[6] Castellano I, Macri L, Deambrogio C, Balmativola D, Bussone R, Ala A, et al. Reliability of whole sentinel lymph node analysis by one-step nucleic acid amplification for intraoperative diagnosis of breast cancer metastases. Ann Surg 2012;255:334–42.

[7] Tamaki Y, Sato N, Homma K, Takabatake D, Nishimura R, Tsujimoto M, et al. Routine clinical use of the one-step nucleic acid amplification assay for detection of sentinel lymph node metastases in breast cancer patients: results of a multicenter study in Japan. Cancer 2012:3477–83.

[8] Visser M, Jiwa M, Horstman A, Brink AA, Pol RP, van Diest P, et al. Intra-operative rapid diagnostic method based on CK19 mRNA expression for the detection of lymph node metastases in breast cancer. Int J Cancer 2008;122: 2562–7.

[9] Schem C, Maass N, Bauerschlag DO, Carstensen MH, Loning T, Roder C, et al. One-step nucleic acid amplification-a molecular method for the detection of lymph node metastases in breast cancer patients; results of the German study group. Virchows Arch 2009;454:203–10.

[10] Khaddage A, Berremila SA, Forest F, Clemenson A, Bouteille C, Seffert P, et al. Implementation of molecular intra-operative assessment of sentinel lymph node in breast cancer. Anticancer Res 2011;31:585–90.

[11] Le Frere-Belda MA, Bats AS, Gillaizeau F, Poulet B, Clough KB, Nos C, et al. Diagnostic performance of one-step nucleic acid amplification for intra-operative sentinel node metastasis detection in breast cancer patients. Int J Cancer 2012;130:2377–86.

[12] Bernet L, Cano R, Martinez M, Duenas B, Matias-Guiu X, Morell L, et al. Diagnosis of the sentinel lymph node in breast cancer: a reproducible molecular method: a multicentric Spanish study. Histopathology 2011;58:863–9.

[13] Snook KL, Layer GT, Jackson PA, de Vries CS, Shousha S, Sinnett HD, et al. Multicentre evaluation of intraoperative molecular analysis of sentinel lymph nodes in breast carcinoma. Br J Surg 2011;98:527–35.

[14] Feldman S, Krishnamurthy S, Gillanders W, Gittleman M, Beitsch PD, Young PR, et al. A novel automated assay for the rapid identification of metastatic breast carcinoma in sentinel lymph nodes. Cancer 2011;117: 2599–607.

[15] Osako T, Iwase T, Kimura K, Yamashita K, Horii R, Yanagisawa A, et al. Intra-operative molecular assay for sentinel lymph node metastases in early stage

breast cancer: a comparative analysis between one-step nucleic acid ampli-fication whole node assay and routine frozen section histology. Cancer 2011;117:4365–74.

[16] Godey F, Leveque J, Tas P, Gandon G, Poree P, Mesbah H, et al. Sentinel lymph node analysis in breast cancer: contribution of one-step nucleic acid ampli-fication (OSNA). Breast Cancer Res Treat 2012;131:509–16.

[17] Vegue LB, Rojo F, Hardisson D, Iturriagagoitia AC, Panades MJ, Velasco A, et al. Comparison of molecular analysis and histopathology for axillary lymph node staging in primary breast cancer: results of the B-CLOSER-I study. Diagn Mol Pathol 2012;21:69–76.

[18] Vilardell F, Novell A, Martin J, Santacana M, Velasco A, Diez-Castro MJ, et al. Importance of assessing CK19 immunostaining in core biopsies in patients subjected to sentinel node study by OSNA. Virchows Arch 2012;460:569–75.

[19] Weaver DL, Ashikaga T, Krag DN, Skelly JM, Anderson SJ, Harlow SP, et al. Effect of occult metastases on survival in node-negative breast cancer. N Engl J Med 2011;364:412–21.

[20] Giuliano AE, Hunt KK, Ballman KV, Beitsch PD, Whitworth PW, Blumencranz PW, et al. Axillary dissection vs no axillary dissection in women with invasive breast cancer and sentinel node metastasis: a randomized clinical trial. JAMA 2011;305:569–75.

[21] Osako T, Iwase T, Kimura K, Yamashita K, Horii R, Akiyama F. Accurate staging of axillary lymph nodes from breast cancer patients using a novel molecular method. Br J Cancer 2011;105:1197–202.

[22] Takeshita T, Tsuda H, Moriya T, Yamasaki T, Asakawa H, Ueda S, et al. Clinical implications of occult metastases and isolated tumor cells in sentinel and non-sentinel lymph nodes in early breast cancer patients: serial step section analysis with long-term follow-up. Ann Surg Oncol 2012;19:1160–6.

Molecular detection of lymph node metastasis in breast cancer patients treated with preoperative systemic chemotherapy: a prospective multicentre trial using the one-step nucleic acid amplification assay

T Osako[1,2], H Tsuda[3], R Horii[2], T Iwase[4], H Yamauchi[5], H Yagata[5], K Tsugawa[5,6], K Suzuki[7], T Kinoshita[8], F Akiyama[*,1] and S Nakamura[5,9]

[1]Division of Pathology, The Cancer Institute of Japanese Foundation for Cancer Research, Tokyo, Japan; [2]Department of Pathology, The Cancer Institute Hospital of Japanese Foundation for Cancer Research, Tokyo, Japan; [3]Department of Pathology and Clinical Laboratories, National Cancer Center Hospital, Tokyo, Japan; [4]Breast Oncology Center, The Cancer Institute Hospital of Japanese Foundation for Cancer Research, Tokyo, Japan; [5]Department of Breast Surgical Oncology, St Luke's International Hospital, Tokyo, Japan; [6]Division of Breast and Endocrine Surgery, St Marianna University School of Medicine, Kanagawa, Japan; [7]Department of Diagnostic Pathology, St Luke's International Hospital, Tokyo, Japan; [8]Breast Surgery Division, National Cancer Center Hospital, Tokyo, Japan and [9]Department of Surgery, Division of Breast Surgical Oncology, Showa University School of Medicine, Tokyo, Japan

Background: For patients with breast cancer treated with preoperative chemotherapy, residual tumour burden in lymph nodes is the strongest prognostic factor. However, conventional pathological examination has limitations that hinder the accurate and reproducible measurement. The one-step nucleic acid amplification (OSNA) assay is a novel molecular method for detecting nodal metastasis. In this prospective multicentre trial, we assessed the performance of the OSNA assay in detecting nodal metastasis after chemotherapy.

Methods: In total, 302 lymph nodes from 80 breast cancer patients who underwent axillary dissection after chemotherapy were analysed. Each node was cut into two or four slices. One piece or alternate pieces were evaluated by pathology, and the other(s) were examined using the OSNA assay. The results of the two methods were compared. Stromal fibrosis, histiocytic aggregates, and degenerated cancer cells were regarded as chemotherapy-induced histological changes.

Results: The overall accuracy, sensitivity, and specificity of the OSNA assay compared with the reference pathology were 91.1%, 88.3%, and 91.7%, respectively. Of the 302 lymph nodes, 66 (21.9%) exhibited chemotherapy-induced histology. For these nodes, the accuracy, sensitivity, and specificity were 90.9%, 88.9%, and 93.3%, respectively.

Conclusion: The OSNA assay can detect the residual tumour burden as accurately as conventional pathology, although chemotherapy-induced histological changes are present.

Preoperative systemic chemotherapy, initially used only for inflammatory and inoperable locally advanced breast cancer, has recently been more widely used for operable disease (Kaufmann et al, 2006; Gralow et al, 2008). Although systemic chemotherapy before and after surgery results in identical survival rates, preoperative chemotherapy has the advantages of eliciting a tumour response in individual patients and increasing the number of patients eligible for breast-conserving surgery (Kaufmann et al, 2006; Gralow et al, 2008). The residual tumour burden in the breast and axillary lymph node after preoperative chemotherapy is the strongest prognostic factor (Carey et al, 2005; von Minckwitz et al, 2012). Moreover, the residual tumour burden in the axillary node is a better prognostic factor than the response of the primary tumour (Rouzier et al, 2002; von Minckwitz et al, 2012), and residual micrometastatic disease is predictive of poor prognosis (Fisher et al, 2002; Klauber-DeMore et al, 2006; Sakakibara et al, 2009). Thus, accurate evaluation of axillary node status is of great clinical significance in patients with breast cancer who are treated with preoperative chemotherapy.

Conventional pathological examination of lymph nodes has three potential limitations that affect the accurate and reproducible measurement of the total residual metastatic volume. First, pathological examinations only partially evaluate each node, and this may lead to underestimation of the nodal status. Although underestimation of the metastasis volume can be reduced by serial sectioning, this imposes a heavy workload for pathologists. Second, histological changes caused by chemotherapy, such as decreases in cellularity with stromal fibrosis, aggregates of foamy histiocytes, and degenerated cancer cells, can affect tumour burden assessment (Sahoo and Lester, 2009). Finally, the practice of pathological evaluation of lymph nodes is not standardised. Examination protocols vary from one institution to another (Cserni et al, 2004), and there is inter-observer variability in diagnosing the tumour burden, particularly for low-volume metastasis (Cserni et al, 2008).

The one-step nucleic acid amplification (OSNA) assay is a novel molecular method for the lymph node staging of breast cancer (Tsujimoto et al, 2007) that has been tested in multiple series (Cserni, 2012; Tamaki, 2012). The results of this semi-automated molecular assay based on the quantification of cytokeratin 19 (CK19) mRNA display a 96% concordance rate with detailed pathology complemented by immunohistochemistry when alternate slices of the same lymph node are used for the two tests (Cserni, 2012; Tamaki, 2012). The OSNA assay is accepted and routinely used in >230 institutions in Spain, Japan, Italy, the UK, France, and other countries (http://lifescience.sysmex.co.jp/ls/products/osna/index.html). However, the performance of the OSNA assay has not been evaluated in patients treated with preoperative systemic therapy. This assay can potentially contribute to the accurate, reproducible, and standardised evaluation of the lymph node status after systemic therapy. In this prospective multicentre trial, we compared the performance of the OSNA assay with that of pathological examination and investigated the effect of chemotherapy-induced histological changes on its performance.

MATERIALS AND METHODS

Enrolled patients and lymph nodes. Axillary lymph nodes were obtained from patients with breast cancer who underwent standard preoperative chemotherapy followed by axillary lymph node dissection between May 2010 and March 2011 at one of three Japanese institutions. This study was approved by the ethics committee of each institution. Patients were given the necessary written information about the study, and only the lymph nodes from patients who gave their consent were included in the analysis.

A maximum of four lymph nodes sampled from the level-I axillary region were included for a single patient. The remaining nodes were evaluated by permanent histology using single-sectioned nodes. The clinical and pathological TNM classification and staging and the level of axillary lymph node dissection of each patient were classified according to the seventh edition of the American Joint Committee on Cancer Staging Manual (Edge et al, 2010).

Lymph node examination process. Sampled fresh lymph nodes larger than 4 mm in short axis were immediately sliced using the cutting device developed by Tsujimoto et al (2007), resulting in two 2-mm central sections (i.e., sections b and c) with additional two excess sections on both sides (i.e., sections a and d; Figure 1A). Alternate pieces (i.e., sections a and c) were evaluated by two-level pathological examination, and the others (i.e., sections b and d) were examined using the OSNA assay. Lymph nodes sized 4 mm or less in short axis were cut by the cutting device into two pieces (Figure 1B). One piece (i.e., section a') was evaluated by pathological examination, and the other piece (i.e., section b') was examined using the OSNA assay. The lymph node slices for pathological examination were fixed with formalin and embedded in paraffin, and the slices for the OSNA assay were stored frozen at − 80 °C until measurement.

Pathological examination. A pair of 4-μm-thick sections was prepared from each slice (Figure 1): one section was stained with haematoxylin-and-eosin and the other was immunostained with a CK19 antibody (Clone RCK108; Dako, Glostrup, Denmark). All slides were centrally reviewed by one experienced pathologist (RH) who was blinded to the results of the OSNA assay. Each node was classified as having macrometastasis (>2.0 mm in size), micrometastasis (>0.2–2.0 mm in size), isolated tumour cells (ITC, ≤0.2 mm in size), or no cancer cells according to the seventh edition of the American Joint Committee on Cancer classification (Edge et al, 2010). Macrometastasis and micrometastasis were regarded as positive findings, and ITCs and no cancer cells were regarded as negative findings. Furthermore, stromal fibrosis, aggregates of foamy histiocytes, and degenerated cancer cells in lymph nodes were regarded as chemotherapy-induced histological changes.

The OSNA assay. The procedure for the OSNA assay has been previously described in detail (Tsujimoto et al, 2007). Briefly, frozen slices of lymph nodes were homogenised with 4 ml of lysis buffer solution (Lynorhag; Sysmex Corporation, Kobe, Japan) and
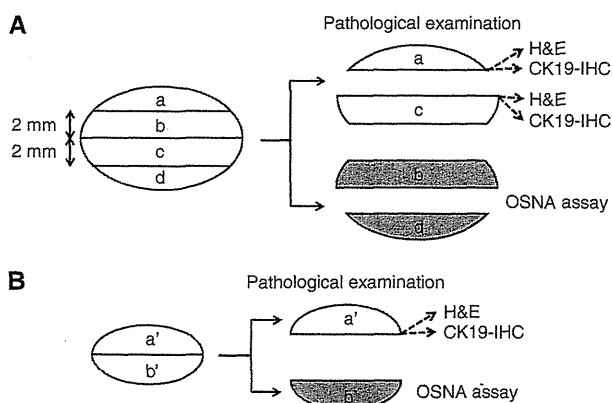

Figure 1. Lymph node examination process. Lymph nodes larger than 4 mm were sliced into four pieces (A), and lymph nodes sized 4 mm or less were cut into two pieces (B). H&E, haematoxylin-and-eosin staining; CK19-IHC, cytokeratin 19 immunohistochemistry; OSNA, one-step nucleic acid amplification.

centrifuged at 10 000 g at room temperature. Two microlitres of supernatant was analysed using the RD-100*i* System (Sysmex Corporation), an automated molecular detection system that uses a reverse transcription loop-mediated isothermal amplification method (Notomi *et al*, 2000), and the LynoampBC Kit (Sysmex Corporation). The degree of amplification was determined on the basis of a reaction by-product, pyrophosphate (Mori *et al*, 2001). The resultant change in turbidity on the precipitation of magnesium pyrophosphate was then correlated with the CK19 mRNA copy number per microlitre of the original lysate via a standard curve established beforehand using three calibrators containing different CK19 mRNA copy numbers. The number of CK19 mRNA copies per microlitre was extrapolated from the standard curve for both the measurement sample and a 1:10 diluted sample. The cutoffs for negative/positive results and (+)/(+ +) were set at 250 and 5000 copies per microlitre, respectively (Tsujimoto *et al*, 2007). Positive (+) was considered equivalent to micrometastasis (not including ITC), and positive (+ +) was considered equivalent to macrometastasis (Tsujimoto *et al*, 2007). In situations in which the reaction was inhibited in the measurement sample, the copy numbers in the diluted sample were used.

Additional investigation of discordant lymph nodes. For lymph nodes that were positive on the OSNA assay and negative (no cancer cells) on pathological examination, the paraffin blocks of the lymph node tissue were step-sectioned with 0.2-mm intervals until the tissue was exhausted. At each level, two microscopic slides were made: one was used for haematoxylin-and-eosin staining and the other was used for CK19 immunostaining. All stained slides were microscopically examined by the central pathologist (RH).

Statistical analysis. With the result of the pathological examination as the gold standard, the accuracy, sensitivity, and specificity of the OSNA assay were calculated. The differences in the accuracy, sensitivity, and specificity between lymph nodes with and without chemotherapy-induced histological changes were assessed by the two-population z-test. Confidence intervals (CIs) were set at the 95% level. P-values of <0.05 were considered statistically significant. All statistical analyses were performed using R statistical software (version 2.10.1, http://www.r-project.org/; Ihaka and Gentleman, 1996).

RESULTS

Enrolled patients and lymph nodes. In total, 307 lymph nodes obtained from 80 patients who underwent surgery after pre-operative chemotherapy were included in the study. Of these, four nodes were excluded because of a lack of lymph node tissue, and one node was excluded because it was not subjected to the OSNA assay. Thus, 302 nodes from 80 patients were included in the analysis. The characteristics of the 80 patients are shown in Table 1. Of the 80 patients, 71 (88.8%) were diagnosed with node-positive before receiving chemotherapy. Of the 71 patients, 8, 52, and 11 were confirmed as positive by sentinel node biopsy, fine needle aspiration cytology, and clinical examination/imaging, respectively. The mean and median numbers of enrolled lymph nodes included from a single patient were 3.8 and 4, respectively. Of the 302 nodes, 192 nodes (63.6%) were sliced into four pieces, and 110 nodes (36.4%) were cut into two pieces.

Overall performance of the OSNA assay. The results of the pathological examination and the OSNA assay were concordant for 275 of 302 nodes (accuracy, 91.1%; 95% CI, 87.3–94.0%; Table 2). Of the 60 nodes identified as positive for metastasis on pathological examination, 53 nodes were identified as positive on the OSNA

Table 1. Patient characteristics

Characteristics	No.	%
No. of patients	80	100.0%
Age (years)		
Median (range)	52 (30–71)	
Clinical N status before chemotherapy		
cN0	9	11.3%
cN1	59	73.8%
cN2	2	2.5%
cN3	10	12.5%
Clinical stage before chemotherapy		
IIA	15	18.8%
IIB	39	48.8%
IIIA	12	15.0%
IIIB	3	3.8%
IIIC	9	11.3%
IV	2	2.5%
Histological type		
Invasive ductal	78	97.5%
Invasive micropapillary	2	2.5%
Oestrogen receptor status		
−	25	31.3%
+	55	68.8%
Progesterone receptor status		
−	38	47.5%
+	42	52.5%
HER2 status		
−	54	67.5%
+	18	22.5%
Uncertain	8	10.0%
Chemotherapy regimen		
Anthracycline	4	5.0%
Anthracycline/taxane	50	62.5%
Anthracycline/taxane/carboplatin	3	3.8%
Anthracycline/taxane/trastuzumab	15	18.8%
Taxane	7	8.8%
Taxane/trastuzumab	1	1.3%
Breast surgery		
Total mastectomy	47	58.8%
Partial mastectomy	33	41.3%
Axillary lymph node dissection		
Level I	1	1.3%
Level II	70	87.5%
Level III	9	11.3%
No. of lymph nodes removed		
Median (range)	16 (5–38)	
Pathological T status after chemotherapy		
ypT0	8	10.0%
ypTis	10	12.5%
ypT1	21	26.3%
ypT2	20	25.0%
ypT3	21	26.3%
Pathological N status after chemotherapy		
ypN0	32	40.0%
ypN1	35	43.8%
ypN2	7	8.8%
ypN3	6	7.5%

Abbreviation: HER2 = human epidermal growth factor receptor-2.